RADIATIVE DECAYS OF THE B MESON: A PROGRESS REPORT*

Mikołaj Misiak

Institute of Theoretical Physics, Faculty of Physics, University of Warsaw
Pasteura 5, 02-093 Warszawa, Poland

(Received May 16, 2018)

Bounds on new physics from $\bar{B} \to X_s\,\gamma$ depend on precise calculations of the Standard Model contributions. The expected experimental accuracy at Belle II implies that both the non-perturbative and perturbative effects need to be evaluated more precisely. Here, the status and progress of such calculations is summarized.

DOI:10.5506/APhysPolB.49.1291

1. Introduction

Weak radiative decays of the B mesons are known as sensitive probes of physics beyond the Standard Model (SM). The inclusive $\bar{B} \to X_s\,\gamma$ decay rate for $E_\gamma > E_0$ is well-approximated by the corresponding perturbative decay rate of the b quark

$$\Gamma\left(\bar{B} \to X_s\,\gamma\right) = \Gamma(b \to X_s^p\,\gamma) + \left(\begin{array}{c}\text{non-perturbative}\\ \text{contributions}\end{array}\right), \tag{1}$$

provided E_0 is large ($E_0 \sim m_b/2$) but not too close to the endpoint ($m_b - 2E_0 \gg \Lambda \sim \Lambda_{\rm QCD}$). For $E_0 = 1.6\,\text{GeV} \simeq m_b/3$, the non-perturbative effects are estimated [1, 2] at the $(3 \pm 5)\%$ level[1].

Once particles much heavier than the b quark have been decoupled, the weak interaction Lagrangian $\mathcal{L}_{\rm weak} \sim \sum C_i Q_i$ that is relevant for $\bar{B} \to X_s\,\gamma$ contains eight operators Q_i [3]. Their field content is displayed[2] in Fig. 1.

* Presented at the Cracow Epiphany Conference on Advances in Heavy Flavour Physics, Kraków, Poland, January 9–12, 2018.

[1] This is the effect of $N(E_0)$ as compared to $P(E_0)^{\rm SM}$ in Eq. (D.4) of Ref. [3], where the overall normalization factors come from semileptonic decay measurements.

[2] More operators appear in generic beyond-SM calculations, as well as in the SM one at subleading orders in $\alpha_{\rm em}$, V_{ub}/V_{cb} or m_s^2/m_b^2.

The corresponding Wilson coefficients C_i at the renormalization scale $\mu_b \sim m_b$ have been determined up to $\mathcal{O}(\alpha_s^2)$ corrections, which required evaluating four-loop anomalous dimension matrices [4].

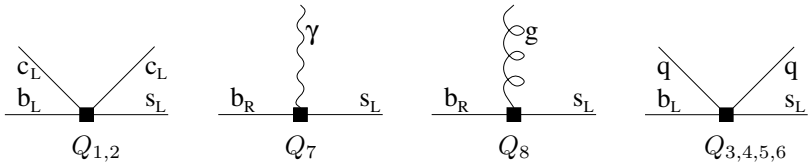

Fig. 1. Field content of the relevant operators.

2. Non-perturbative effects in $\bar{B} \to X_s\gamma$

To discuss non-perturbative effects in the decay rate, it is convenient to begin with the leading contribution that is proportional to $|C_7|^2$. We write

$$\Gamma\left(\bar{B} \to X_s\gamma\right)_{E_\gamma > E_0} = |C_7(\mu_b)|^2\, \Gamma_{77}(E_0) + (\text{other})\,. \tag{2}$$

The derivative of Γ_{77} with respect to the photon energy can be related via the optical theorem to the forward $\bar{B}\gamma \to \bar{B}\gamma$ scattering amplitude A generated by Q_7 alone (see the left plot of Fig. 2)

$$\frac{\mathrm{d}\Gamma_{77}}{\mathrm{d}E_\gamma} \sim \mathrm{Im}A\,. \tag{3}$$

To evaluate $\Gamma_{77}(E_0)$, we need to integrate $\mathrm{Im}A$ from E_0 to $E_{\max} \simeq m_B/2$. We can do it by considering E_γ as complex, and realizing that $\mathrm{Im}A$ is proportional to the discontinuity of A at the branch cut indicated by the thick (blue) line on the real axis in the right plot of Fig. 2. Instead of integrating along this line, we can use the circular contour shown in the plot. If $m_b - 2E_0 \gg \Lambda$, the intermediate hadronic state X_s is far off shell on the whole circle, and an operator product expansion can be applied. In consequence, $\Gamma_{77}(E_0)$ can be expressed in terms of matrix elements of local operators between $\bar{B}$ meson states at rest, with perturbatively calculable coefficients. The leading contribution reproduces the perturbative result [5–7], while the non-perturbative corrections form a series in powers of Λ/m_b, $\Lambda/(m_b - 2E_0)$ and α_s that begins with

$$\frac{\mu_\pi^2}{m_b^2}\,, \qquad \frac{\mu_G^2}{m_b^2}\,, \qquad \frac{\rho_D^3}{m_b^3}\,, \qquad \frac{\rho_{LS}^3}{m_b^3}\,, \qquad \frac{\alpha_s\mu_\pi^2}{(m_b - 2E_0)^2}\,, \qquad \frac{\alpha_s\mu_G^2}{m_b(m_b - 2E_0)}\,, \tag{4}$$

where $\mu_\pi, \mu_G, \rho_D, \rho_{LS} = \mathcal{O}(\Lambda)$ are extracted from the semileptonic $\bar{B} \to X_c e \bar{\nu}$ spectra and the $B - B^\star$ mass difference (see Ref. [8] for the most recent fits). Perturbative coefficients at the quantities listed in Eq. (4) were evaluated in Refs. [7, 9–11]. With these inputs, $\Gamma_{77}(E_0)$ is a precisely known contribution to the decay rate.

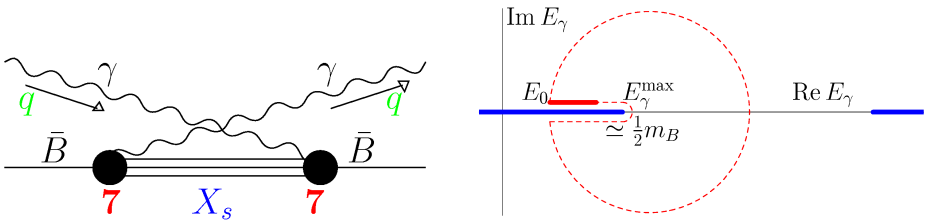

Fig. 2. Left: The amplitude A in Eq. (3). Right: Contour integrals of A (see the text).

The main non-perturbative uncertainty arises from the so-called resolved photon contributions where the b-quark annihilation vertex and the photon emission vertex are not necessarily close to each other in space (as compared to $\mathcal{O}(1/\Lambda)$). Such contributions arise, for instance, in the $Q_{1,2}$–Q_7 interference. If the charm quark mass squared was larger than $\mathcal{O}(m_b\Lambda)$, we could express the corresponding relative contribution to the CP- and isospin-averaged $\bar{B} \to X_s\gamma$ branching ratio $\mathcal{B}_{s\gamma}$ as [1, 12–15]

$$\frac{\Delta\mathcal{B}_{s\gamma}}{\mathcal{B}_{s\gamma}} = -\frac{6C_2(\mu_b) - C_1(\mu_b)}{18C_7(\mu_b)} \left[\frac{\mu_G^2}{m_c^2} + \sum_n b_n \mathcal{O}\left(\frac{\Lambda^2}{m_c^2}\left(\frac{m_b\Lambda}{m_c^2}\right)^n\right)\right], \qquad (5)$$

where $\mu_G^2 \simeq 0.31\,\text{GeV}^2$ [8], and the coefficients b_n decrease fast with n. However, as pointed out in Ref. [2], one cannot trust expansion (5) so long as m_c^2 is not really much larger than $\mathcal{O}(m_b\Lambda)$, *i.e.* the B-meson wave function contains a significant fraction of gluons with momenta of the order of m_c^2/m_b. Instead, the considered contribution was treated in Ref. [2] as a $\mathcal{O}(\Lambda/m_b)$ one, and estimated using models of the so-called soft functions, within the formalism of Soft Collinear Effective Theory. The same method was applied to the Q_7–Q_8 and Q_8–Q_8 interferences that contain $\mathcal{O}(\Lambda/m_b)$ effects from resolved photons, too. Dominant contributions to the estimated non-perturbative uncertainty in $\mathcal{B}_{s\gamma}$ were found this way. Relatively strong experimental constraints on moments of the considered soft functions still allow them to have sizeable tails towards larger gluon momenta, provided one's attention is not restricted to functions of a definite sign.

It is worth noting that non-perturbative effects in the Q_8–Q_8 interference contain contributions that are not suppressed by Λ/m_b [16, 17]. Their presence is signalled by collinear divergences (regularized by $m_s \neq 0$) in the corresponding perturbative expressions. Similar effects are observed in matrix elements of the penguin operators [18, 19]. In such cases, an appropriate approach amounts to employing experimentally determined fragmentation functions to estimate photon emission probabilities from jets corresponding to particular partons. Fortunately, such effects are absent in the major contributions to $\mathcal{B}_{s\gamma}$ that either involve the photonic dipole operator or are due to the $Q_{1,2}$–$Q_{1,2}$ interferences. In consequence, the collinear effects have only a small contribution to the overall non-perturbative uncertainty in $\mathcal{B}_{s\gamma}$.

Relative contributions to $\mathcal{B}_{s\gamma}$ from various interference terms are plotted in Fig. 3 as functions of μ_b. They are normalized in such a way that they sum to unity for each μ_b. They have been evaluated as in the phenomenological analysis of Refs. [3, 20], including estimated central values for non-perturbative effects. One can see that the Q_7–Q_7 and $Q_{1,2}$–Q_7 interference terms are by far the dominant. On the other hand, those where the collinear effects are present never exceed 1% of the total rate. It is due to several reasons, including sizes of the Wilson coefficients, $\alpha_s(\mu_b)$, phase-space suppression for $E_0 \sim m_b/3$, as well as factors like $Q_d^2 = 1/9$ (the square of the down quark electric charge).

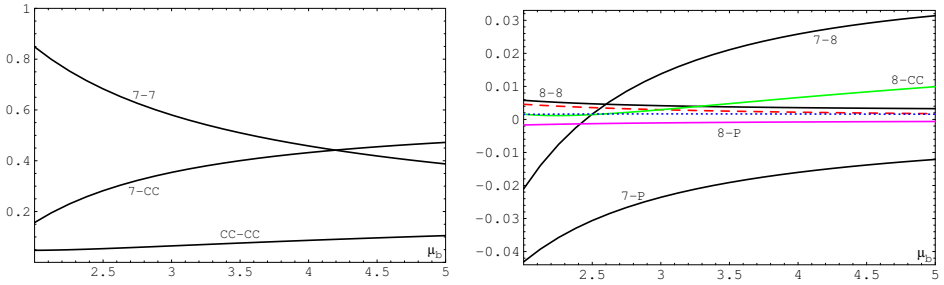

Fig. 3. Relative contributions to $\mathcal{B}_{s\gamma}$ from various interference terms as functions of μ_b. The symbols CC and P stand for the current–current and penguin operators, respectively. The dashed (red) and dotted (blue) curves describe the P–P and P–CC interferences, respectively.

As far as the dependence of $\mathcal{B}_{s\gamma}$ on the scale μ_b is concerned, it is much weaker than for the individual contributions here — see Fig. 6 of Ref. [3]. Once all the perturbative contributions are evaluated up to $\mathcal{O}(\alpha_s^2)$ and added together, such a dependence in $\Gamma(b \to X_s^p \gamma)$ becomes a higher-order ($\mathcal{O}(\alpha_s^3)$) effect.

3. Calculations of perturbative contributions

As suggested in Ref. [21], it is convenient to fix the overall normalization in the theoretical prediction for $\mathcal{B}_{s\gamma}$ with the help of quantities extracted from the semileptonic decay measurements, namely the inclusive branching ratio $\mathcal{B}(\bar{B} \to X_c \ell \bar{\nu})$, and the so-called semileptonic phase-space factor $C = |V_{ub}/V_{cb}|^2 \, \mathcal{B}(\bar{B} \to X_c \ell \bar{\nu})/\mathcal{B}(\bar{B} \to X_u \ell \bar{\nu})$. In such a case, the relevant perturbative quantity to be considered is

$$\frac{\Gamma[b \to X_s \gamma]_{E_\gamma > E_0}}{\Gamma[b \to X_u e \bar{\nu}]} = \left| \frac{V_{ts}^* V_{tb}}{V_{ub}} \right|^2 \frac{6\alpha_{\rm em}}{\pi} \sum_{i,j} C_i(\mu_b) \, C_j(\mu_b) \, K_{ij} \, . \tag{6}$$

Both K_{ij} and $C_i(\mu_b)$ are evaluated order-by-order in $\widetilde{\alpha}_{\rm s} \equiv \frac{\alpha_{\rm s}(\mu_b)}{4\pi}$

$$C_i(\mu_b) \;=\; C_i^{(0)} + \widetilde{\alpha}_{\rm s} \, C_i^{(1)} + \widetilde{\alpha}_{\rm s}^2 \, C_i^{(2)} + \ldots \, , \tag{7}$$

$$K_{ij} \;=\; K_{ij}^{(0)} + \widetilde{\alpha}_{\rm s} \, K_{ij}^{(1)} + \widetilde{\alpha}_{\rm s}^2 \, K_{ij}^{(2)} + \ldots \tag{8}$$

All the explicitly displayed terms in the above expansions are now known in a complete manner, except for several Next-to-Next-to-Leading Order (NNLO) quantities $K_{ij}^{(2)}$. Among the incompletely known NNLO corrections, the most important ones are $K_{27}^{(2)}$ and $K_{17}^{(2)}$. Their dependence on $z = \frac{m_c^2(\mu_c)}{m_b^2}$ and $\delta = 1 - \frac{2E_0}{m_b}$ can be expressed as follows:

$$K_{27}^{(2)}(z,\delta) \;=\; A_2 + F_2(z,\delta) - \tfrac{27}{2} f_q(z,\delta) + f_b(z) + g_c(z,\delta) + \ldots \, , \tag{9}$$

$$K_{17}^{(2)}(z,\delta) \;=\; -\tfrac{1}{6} K_{27}^{(2)}(z,\delta) + A_1 + F_1(z,\delta) + \ldots \, , \tag{10}$$

where ellipses stand for terms proportional to $\ln(\mu_b/m_b)$, $\ln^2(\mu_b/m_b)$, $\ln(\mu_c/m_c)$, or vanishing in the limit $m_b \to m_b^{\rm pole}$. The functions f_b, g_c and f_q originate, respectively, from diagrams with closed loops of the bottom, charm and light (u, d, s) quarks on the gluon lines [22–24]. The masses of the light quarks have been neglected, and the coefficient at f_q has been adjusted in such a manner that the terms accounted for in the Brodsky–Lepage–Mackenzie (BLM) approximation [25] do not affect $A_i + F_i(z,\delta)$.

The functions $F_i(z,\delta)$ stand for those NNLO contributions to $K_{i7}^{(2)}$ whose dependence on z and δ remains unknown. The additive constants A_i are fixed by imposing $F_i(0,1) = 0$. In Ref. [3], an explicit calculation of the considered corrections was performed at $z = 0$ and $\delta = 1$. It gave $A_1 \simeq 22.605$ and $A_2 \simeq 75.603$. Next, the functions $F_i(z,\delta)$ were estimated using an interpolation of $F_i(z,1)$ in z between $F_i(0,1) = 0$ and the asymptotic large-z expressions determined in Ref. [26]. The interpolated functions were

assumed to be linear combinations of $f_q(z,1)$, $K_{27}^{(1)}(z,1)$, $z\frac{\mathrm{d}}{\mathrm{d}z}K_{27}^{(1)}(z,1)$ and a constant term. The boundary conditions at $z=0$ and at large z were sufficient to determine such linear combinations in a unique manner. Our choice of the four functions for the interpolation was motivated by the fact that all the effects due to renormalization in the considered corrections are proportional to these very functions.

The interpolated correction turns out to affect $\mathcal{B}_{s\gamma}$ by around 5%, with an uncertainty estimated at the ±3% level. This uncertainty is added in quadrature to the remaining ones that stem from non-perturbative effects (±5%), order-α_s^3 corrections (±3%), and parametric uncertainties (±2%). With such estimates, the SM prediction for $\mathcal{B}_{s\gamma}$ at $E_0 = 1.6\,\mathrm{GeV}$ amounts to $\mathcal{B}_{s\gamma}^{\mathrm{SM}} = (3.36 \pm 0.23) \times 10^{-4}$ [3, 20]. It agrees very well with the current experimental average $\mathcal{B}_{s\gamma}^{\mathrm{exp}} = (3.32 \pm 0.15) \times 10^{-4}$ [27] that is based on measurements of CLEO [28], Belle [29, 30] and BaBar [31–33]. The present (±4.5%) experimental uncertainty is going to be reduced to $\mathcal{O}(3\%)$ level with the full Belle II dataset [34].

Further improvements in the accuracy of determining the perturbative contribution to $\mathcal{B}_{s\gamma}$ require an actual evaluation of $F_i(z,1)$ for the physical value of z. Next, one should extend the calculation to $\delta \neq 1$ by considering the photon energy spectrum away from the endpoint, as in the first calculations of $K_{77}^{(2)}$ [35, 36].

Following the approach of the $z=0$ calculation in Ref. [3], $F_i(z,1)$ can be determined from four-loop propagator diagrams with unitarity cuts. Examples of such diagrams are shown in Fig. 4. The corresponding counterterm contributions have been already evaluated in Ref. [37]. As far as the bare contributions are concerned, one begins with generation of diagrams and expressing the considered Q_7–$Q_{1,2}$ interference in terms of 585 309 scalar integrals in 437 families. All these integrals are linear combinations of a few hundreds of Master Integrals (MIs), with coefficients being rational functions of z. Finding the MIs and the corresponding coefficients requires generating and solving large numbers of linear equations that stem from Integration By Parts (IBP). So far, the program FIRE [38] has been used for this purpose, with symmetries supplied by LiteRed [39, 40]. For the most complicated families, $\mathcal{O}(1\,\mathrm{TB})$ of RAM and weeks of CPU are necessary at the moment, which calls for further optimization of the algorithms.

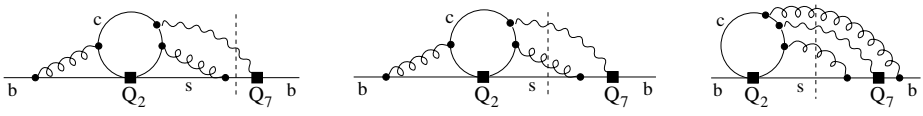

Fig. 4. Sample diagrams for $F_i(z,1)$ with unitarity cuts indicated by the dashed lines.

Once the IBP reduction is over (hopefully soon), a closed set of Differential Equations (DEs) can be derived for each family of the MIs. Such equations take the form of

$$\frac{\mathrm{d}}{\mathrm{d}z} I_n(z,\epsilon) = \sum_k w_{nk}(z,\epsilon)\, I_k(z,\epsilon)\,, \tag{11}$$

where I_n stand for the MIs, while $w_{nk}(z,\epsilon)$ are certain rational functions obtained from the IBP reduction. Boundary conditions for the DEs at large z are, in principle, much easier to calculate than the MIs themselves. However, their calculation must be fully automatic, due to the large numbers of the MIs involved. Next, the DEs can be solved numerically along ellipses in the complex z plane. Such an approach has been already successfully applied for the counterterm contributions in Ref. [37].

The ultimate goal of such calculations is suppressing the purely perturbative uncertainties roughly twice with respect to the current estimates. This should give sufficient motivation for reconsidering the non-perturbative resolved photon contributions, in which case the current state of art is still given by the 2010 analysis of Ref. [2].

4. Bounds on the 2HDM parameters

As mentioned in the previous section, the current SM prediction for $\mathcal{B}_{s\gamma}$ is in a very good agreement with the experimental average. This fact leads to strong constraints on many interesting extensions of the SM. Here, we shortly discuss constraints on the Two-Higgs-Doublet Model (2HDM), following the analysis of Ref. [41]. In that paper, the quantity $R_\gamma = (\mathcal{B}_{s\gamma} + \mathcal{B}_{d\gamma})\,/\mathcal{B}_{c\ell\nu}$ was used instead of $\mathcal{B}_{s\gamma}$, which slightly improves the sensitivity. Plots of R_γ as functions of the charged Higgs boson mass $M_{H^\pm}$ in two most popular versions of the 2HDM, the so-called Model I and Model II, are shown in Fig. 5. At large $M_{H^\pm}$, they tend to the SM prediction $R_\gamma^{\mathrm{SM}} = (3.31 \pm 0.22) \times 10^{-3}$. One can see that the plotted 2HDM predictions begin to significantly differ from the experimental results (dotted lines) for $M_{H^\pm}$ as heavy as 500–700 GeV. The two plots shown in Fig. 5 correspond to particular values of $\tan\beta$, the ratio of vacuum expectation values of the two scalar doublets. In the case of Model I, the plot corresponds to $\tan\beta = 1$, while $\tan\beta = 50$ has been used for Model II. In the latter model, R_γ is a sum of two positive terms, one of which is independent of $\tan\beta$, and the other one is proportional to $\cot^2\beta$ (becoming negligible for $\tan\beta = 50$). In consequence, R_γ gives us an absolute ($\tan\beta$-independent) bound on $M_{H^\pm}$ in Model II. The actual value of this bound depends on details of its derivation, as elaborated in Ref. [41]. A conservative approach leads to $M_{H^\pm} > 580\,\mathrm{GeV}$ at 95% C.L.

As far as Model I is concerned, we have $R_\gamma \sim \cot^2\beta$. In consequence, relevant bounds on $M_{H^\pm}$ are obtained for $\tan\beta \lesssim 2$ only. For $\tan\beta = 1$, one finds $M_{H^\pm} > 445\,\text{GeV}$ at 95% C.L.

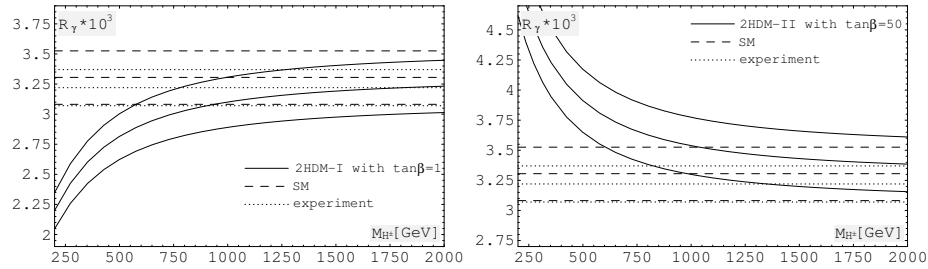

Fig. 5. R_γ at $E_0 = 1.6\,\text{GeV}$ as a function of $M_{H^\pm}$ in Model I with $\tan\beta = 1$ (left) and in Model II with $\tan\beta = 50$ (right). Middle lines show the central values, while the upper and lower ones are shifted by $\pm 1\sigma$. Solid and dashed curves correspond to the 2HDM and SM predictions, respectively. Dotted lines show the experimental average $R_\gamma^{\text{exp}} = (3.22 \pm 0.15) \times 10^{-3}$.

5. Summary

Uncertainties in the SM prediction for $\mathcal{B}_{s\gamma}$ originate from perturbative and non-perturbative effects. Improvements in accuracy are necessary in both cases to match the current and future experimental precision. In the perturbative case, the main issue is replacing estimates of the NNLO corrections that are based on interpolation in m_c by actual calculations at the physical value of m_c. In the non-perturbative case, the resolved photon contributions generate the main uncertainty. One might wonder whether methods applied for estimating charm quark loop effects in the exclusive $B \to K^* \ell^+ \ell^-$ decays could be useful for $\bar{B} \to X_s\gamma$.

As far as constraints on beyond-SM physics are concerned, the most pronounced bounds from $\mathcal{B}_{s\gamma}$ are obtained for 2HDM II, in which case the charged Higgs boson mass below 580 GeV is excluded at 95% C.L.

This research has been partially supported by the National Science Centre, Poland (NCN) under the research project 2017/25/B/ST2/00191, and through the HARMONIA project under contract UMO-2015/18/M/ST2/00518.

REFERENCES

[1] G. Buchalla, G. Isidori, S.J. Rey, *Nucl. Phys. B* **511**, 594 (1998).

[2] M. Benzke, S.J. Lee, M. Neubert, G. Paz, *J. High Energy Phys.* **1008**, 099 (2010).

[3] M. Czakon *et al.*, *J. High Energy Phys.* **1504**, 168 (2015).

[4] M. Czakon, U. Haisch, M. Misiak, *J. High Energy Phys.* **0703**, 008 (2007).

[5] J. Chay, H. Georgi, B. Grinstein, *Phys. Lett. B* **247**, 399 (1990).

[6] I.I.Y. Bigi, N.G. Uraltsev, A.I. Vainshtein, *Phys. Lett. B* **293**, 430 (1992) [*Erratum ibid.* **297**, 477 (1992)].

[7] I.I.Y. Bigi *et al.*, `arXiv:hep-ph/9212227`.

[8] A. Alberti, P. Gambino, K.J. Healey, S. Nandi, *Phys. Rev. Lett.* **114**, 061802 (2015).

[9] A.F. Falk, M.E. Luke, M.J. Savage, *Phys. Rev. D* **49**, 3367 (1994).

[10] C.W. Bauer, *Phys. Rev. D* **57**, 5611 (1998) [*Erratum ibid.* **60**, 099907 (1999)].

[11] T. Ewerth, P. Gambino, S. Nandi, *Nucl. Phys. B* **830**, 278 (2010).

[12] Z. Ligeti, L. Randall, M.B. Wise, *Phys. Lett. B* **402**, 178 (1997).

[13] A.K. Grant, A.G. Morgan, S. Nussinov, R.D. Peccei, *Phys. Rev. D* **56**, 3151 (1997).

[14] M.B. Voloshin, *Phys. Lett. B* **397**, 275 (1997).

[15] A. Khodjamirian, R. Rückl, G. Stoll, D. Wyler, *Phys. Lett. B* **402**, 167 (1997).

[16] A. Ferroglia, U. Haisch, *Phys. Rev. D* **82**, 094012 (2010).

[17] H.M. Asatrian, C. Greub, *Phys. Rev. D* **88**, 074014 (2013).

[18] M. Kamiński, M. Misiak, M. Poradziński, *Phys. Rev. D* **86**, 094004 (2012).

[19] T. Huber, M. Poradziński, J. Virto, *J. High Energy Phys.* **1501**, 115 (2015).

[20] M. Misiak *et al.*, *Phys. Rev. Lett.* **114**, 221801 (2015).

[21] P. Gambino, M. Misiak, *Nucl. Phys. B* **611**, 338 (2001).

[22] Z. Ligeti, M.E. Luke, A.V. Manohar, M.B. Wise, *Phys. Rev. D* **60**, 034019 (1999).

[23] K. Bieri, C. Greub, M. Steinhauser, *Phys. Rev. D* **67**, 114019 (2003).

[24] R. Boughezal, M. Czakon, T. Schutzmeier, *J. High Energy Phys.* **0709**, 072 (2007).

[25] S.J. Brodsky, G.P. Lepage, P.B. Mackenzie, *Phys. Rev. D* **28**, 228 (1983).

[26] M. Misiak, M. Steinhauser, *Nucl. Phys. B* **840**, 271 (2010).

[27] Y. Amhis *et al.* [Heavy Flavor Averaging Group], `arXiv:1612.07233 [hep-ex]`.

[28] S. Chen *et al.* [CLEO Collaboration], *Phys. Rev. Lett.* **87**, 251807 (2001).

[29] A. Abdesselam *et al.* [Belle Collaboration], `arXiv:1608.02344 [hep-ex]`.

[30] T. Saito *et al.* [Belle Collaboration], *Phys. Rev. D* **91**, 052004 (2015).
[31] J.P. Lees *et al.* [BaBar Collaboration], *Phys. Rev. Lett.* **109**, 191801 (2012).
[32] J.P. Lees *et al.* [BaBar Collaboration], *Phys. Rev. D* **86**, 052012 (2012).
[33] B. Aubert *et al.* [BaBar Collaboration], *Phys. Rev. D* **77**, 051103 (2008).
[34] P. Urquijo, talk presented at the Sixth Workshop on Rare Semileptonic B Decays, Munich, Germany, February 20–22, 2018.
[35] I.R. Blokland *et al.*, *Phys. Rev. D* **72**, 033014 (2005).
[36] K. Melnikov, A. Mitov, *Phys. Lett. B* **620**, 69 (2005).
[37] M. Misiak, A. Rehman, M. Steinhauser, *Phys. Lett. B* **770**, 431 (2017).
[38] A.V. Smirnov, *Comput. Phys. Commun.* **189**, 182 (2015).
[39] R.N. Lee, `arXiv:1212.2685 [hep-ex]`.
[40] A.V. Smirnov, V.A. Smirnov, *Comput. Phys. Commun.* **184**, 2820 (2013).
[41] M. Misiak, M. Steinhauser, *Eur. Phys. J. C* **77**, 201 (2017).